Neurometabolic predictors of mental effort in the frontal cortex

Arthur Barakat[*,1], Nicolas Clairis[*,1,2], Jules Brochard[3], Mathias Pessiglione[4], Jean-Philippe Godin[5], Bernard Cuenoud[6,7] Lijing Xin[8,9], Carmen Sandi[1&]

[1]Laboratory of Behavioral Genetics (LGC), Brain Mind Institute (BMI), École Polytechnique Fédérale de Lausanne (EPFL), Lausanne, Switzerland

[2]Psychiatry Department, Faculty of Medicine, University of Geneva, Geneva, Switzerland

[3]Transdisciplinary Research Areas, Life and Health, University of Bonn, Bonn, Germany

[4]Motivation, Brain and Behavior team, Paris Brain Institute, Sorbonne University, Institut National de la Santé et de la Recherche Médicale, Centre National de la Recherche Scientifique, Paris, France

[5]Nestlé Research, Société des Produits Nestlé SA, Lausanne, Switzerland

[6]Nestlé Health Science, Epalinges, Switzerland

[7]Department of Medicine, Faculty of Medicine and Health Sciences, Université de Sherbrooke, Sherbrooke, Canada

[8]Center for Biomedical Imaging (CIBM), École Polytechnique Fédérale de Lausanne (EPFL), Lausanne, Switzerland

[9]Institute of Physics (IPHYS), École Polytechnique Fédérale de Lausanne (EPFL), Lausanne, Switzerland

* Equal contribution

[&] Corresponding & lead author: carmen.sandi@epfl.ch

Key words: Motivation; effort-based decision-making; mental effort; neurometabolism; ^{1}H-MRS; machine learning; dorsomedial prefrontal cortex; dorsal anterior cingulate cortex; anterior insula

Abstract

Motivation drives individuals to overcome costs to achieve desired outcomes, such as rewards or avoidance of punishment, with significant variability across individuals. The dorsomedial prefrontal cortex/dorsal anterior cingulate cortex (dmPFC/dACC) and anterior insula are key brain regions implicated in effort-based decision-making. Here, we utilized proton magnetic resonance spectroscopy (^{1}H-MRS) at 7 Tesla on 69 healthy participants in these brain regions to uncover the neurometabolic factors that influence these differences. We designed and applied an effort-based decision-making task requiring mental and physical effort to probe motivated behavior, complemented by computational modeling to extract key behavioral parameters. Gradient boosting machine learning was applied to explore the predictive role of specific metabolites in motivated behavior. Our results reveal that a model established on dmPFC/dACC metabolites explains decisions to exert high mental effort and sensitivity to mental effort. In particular, glutamate, aspartate, and lactate in dmPFC/dACC, three metabolites linked through the tricarboxylic acid cycle and glycolysis, were identified as key discriminative metabolites in the dmPFC/dACC, predictive of mental effort choices, underpinning energy supply and cognitive processes. Anterior insula metabolites did not significantly relate to effort-related decisions. Notably, glutamine and lactate levels between the periphery (plasma) and the dmPFC/dACC were correlated, suggesting a metabolic link between peripheral and central biomarkers of effort. Our findings provide novel insights into the neurometabolic underpinnings of motivated behavior and propose novel biomarkers for mental effort-based decision-making. Importantly, our study highlights the relevance of multivariate approaches in elucidating complex cognitive functions.

Introduction

Motivation drives individuals to overcome the inherent costs of actions to achieve desired outcomes, such as obtaining rewards or avoiding punishments [1,2]. This process, fundamental to human behavior, involves making decisions based on cost-benefit trade-offs between the rewards involved in an action and the effort required to reach them. However, there is striking variability in how individuals approach effortful decisions. These inter-individual differences can significantly impact well-being, longevity, and success in life [3–5]. Moreover, a pronounced aversion to effort exertion is a key symptom in various brain pathologies [2,6]. While such diversity in motivational drive reflects a significant aspect of human cognition, our understanding of the neurobiological underpinnings of these inter-individual differences remains limited.

Neurobiologically, motivation and effort-based decision-making are linked to the functioning of the dorsomedial prefrontal cortex/dorsal anterior cingulate cortex (dmPFC/dACC) [2,7–10] which plays a pivotal role in driving mental and physical effort [11–13]. Lesions in this area can lead to increased effort aversion [14] and even akinetic mutism [15], a state characterized by a lack of initiative to act. However, our understanding of the specific neurobiological components within the dmPFC/dACC that influence effort-based decision-making is still limited. Investigating these factors is vital for developing strategies to enhance motivation.

Recent advances emphasize the importance of brain bioenergetic and metabolic processes for brain function, behavior, and cognition [16–18]. Initial studies predominantly focused on glucose as a resource-limiting energy source for demanding cognitive processes [19,20]. However, brain glucose is not the only resource for cognitive processes as was originally proposed [21–24]. Neurons utilize various energy substrates, not just glucose, to support both neural structure and function [25–29] and, consequently, meet cognitive demands [18]. Several animal and human studies suggest that neurometabolic components in different brain regions are involved in decision-making and motivation [30–36]. Accordingly, cognitive processes, including motivation and decision-making, are closely linked to the brain's metabolic state. However, our understanding of how metabolism influences motivational processes and decision-making is still in its early stages.

Magnetic resonance spectroscopy (MRS) enables the non-invasive quantification of brain metabolites thereby providing insights into the neurochemical state of specific brain regions. Proton (^{1}H)-MRS enables the quantification of several brain metabolites, such as glutamate, lactate, aspartate, N-acetylaspartate (NAA), creatine, and others. These metabolites play crucial roles in neuronal health, energy metabolism, and cellular signaling, all key for neural function and behavior production [37–39]. Understanding whether the concentrations of these metabolites in key brain regions are related

to effort-based motivated processes can provide invaluable insights into the neurometabolic foundations of these cognitive functions. Previous human studies have offered initial evidence linking specific metabolites in specific brain regions to individuals' performance in motivation and decision-making tasks [32,34,36,40,41]. However, virtually all the studies linking metabolite concentrations, acquired through ^{1}H-MRS, to behavior or cognition have focused on individual metabolites using univariate analyses, overlooking how the combined influence of multiple metabolites contributes to motivated behavior. Addressing this gap by employing multivariate statistical methods can provide a more comprehensive view of the neurochemical bases of motivated behavior.

In this study, we leveraged the critical role of the dmPFC/dACC in assessing cost-benefit trade-offs to explain individual differences in decision-making for effort-based motivated behavior. We utilized ultra-high field 7 Tesla (7T) ^{1}H-MRS to measure metabolite concentrations in the dmPFC/dACC and in the anterior insula (AI), as the AI that has also been involved in mental and physical effort [2,11,42], and both regions are key nodes of the brain salience network [43]. Additionally, we conducted targeted metabolomic analyses of plasma samples. To gauge participants' willingness to exert physical and mental efforts, we created an effort-based decision-making task where subjects chose between a fixed low effort/low incentive option and a varying high effort/high incentive option. The task involved trials in which participants could obtain rewards or avoid punishment, alternating between mental and physical effort blocks. We applied computational modeling to extract key parameters influencing effortful decisions in our task, such as mental and physical effort perception [2,44]. We subsequently employed machine learning models to explore whether specific dmPFC/dACC and AI metabolite combinations could predict effortful choices and parameters of motivated behavior. Our study offers new insights into how the dmPFC/dACC metabolic processes relate to motivated behavior components, potentially identifying novel biomarkers and therapeutic targets for motivation-related cognitive functions, especially in the context of mental effort and perception.

Methods

Participants

A total of 75 healthy volunteers (40 females) participated in the study, approved by the Cantonal Ethics Committee of Vaud (CER-VD), Switzerland. Data analyzed here is part of a larger study from which a report focusing on physical effort has been previously published [36]. Exclusion criteria included being outside the 25 - 40 years age range, regular drug or medication use, history of neurological disorders, and MRI contraindications. Informed consent was obtained from all participants before being invited to the study. Pre-visit, online questionnaires were completed, including the Montgomery Asberg Depression Rating Scale – self-rated (MADRS-S), with a cutoff of 4 differentiating non-depressive from

mild/high depressive individuals. This ensured a wide behavior range and sufficient inter-individual variability. After exclusion for incomplete or incongruent behavior, the sample included 71 subjects (35 females). See Supplementary Methods for further details.

Experimental procedure

Participants abstained from eating for 1.5 hours before attendance. Blood samples were collected by healthcare professionals at specified locations (i.e., Point Santé" in EPFL and the "Centre Médical des Arcades", Lausanne) followed by baseline metabolite concentration assessments using proton magnetic resonance spectroscopy (^{1}H-MRS) in the dmPFC/dACC and AI (see Fig. 1a-c). Task training occurred outside the scanner, with participants' maximum voluntary contraction (MVC) and maximum number of correct responses (MNCR) determined to calibrate task difficulty. The range of incentives used was calibrated by identifying the indifference points, corresponding to a 50% chance of accepting a certain level of effort for a given monetary incentive [45]. The behavioral task explores different aspects of motivated behavior while capturing a wide range of interindividual differences (Fig. 1d). On every trial, participants were asked to choose between a fixed low incentive/low effort option and a high incentive/high effort option, varying in both effort and incentive levels. After their choice selection, the selected option was displayed by continuous (for high confidence) or dotted (for low confidence) lines reflecting the level of confidence indicated by the subject. After their choice, participants had to perform the corresponding effort chosen. Incentives were either framed as monetary loss or gain. Effort was either physical, implying to exert a force equal or superior to 55 % of the participant's MVC during a varying amount of time depending on the level of effort selected, or mental, implying to perform different numbers of correct responses in a 2-back task, depending on their MNCR. The complete set of explanations is reported in the Supplementary Methods.

MRS acquisition and preprocessing

Proton magnetic resonance (^{1}H-MR) spectra were collected using a 7 Tesla/68 cm MR scanner (Magnetom, Siemens Medical Solutions, Erlangen, Germany) with a single-channel quadrature transmitter and a 32-channel receive coil (Nova Medical Inc., MA, USA). See Supplementary Methods and **Figure S1**) for details.

Computational modeling of motivated behavior

Participants' choices were fitted with a softmax model using Matlab's VBA toolbox (https://mbb-team.github.io/VBA-toolbox/) which implements Variational Bayesian analysis under the Laplace approximation [46]. The details of the model have been described in our previous publication [36], but the details can also be found in the Supplementary Materials & Methods. In brief, the model fits the probability of choosing the high effort option with a sigmoid transformation aiming at extracting

individual parameters reflecting the weight that different task parameters had on decision-making. These parameters included sensitivity to reward (kR), punishment (kP), physical effort (kEp), mental effort (kEm), physical fatigue (kFp), mental learning (kLm) and a bias term (bias) capturing the general propensity to engage with the task. Subsequently, all parameters except the bias term were boxcox transformed to reduce skewness and increase normality [47].

Feature selection and extreme gradient boosting trees (XGBoost)

Feature selection plays a crucial role in developing predictive models, as it simplifies the model by removing redundant features and mitigates overfitting, particularly for small sample sizes with limited generalization ability. Our dataset was first divided in a train/test split, with 80% of the dataset kept for training and 20% for testing. To avoid bias in test predictions, feature selection was conducted on the training dataset for both models. Features with a Pearson correlation coefficient smaller than 0.1 with the target variable were removed. As a second round of feature selection, Sklearn.*AdaBoostRegressor* package was used to train models using approach CVLOO to predict target variables. The selected features were those that yielded the smallest validation error from the CVLOO approach. The resulting metabolites were used to train both machine learning algorithms.

We employed *XGBoost* to predict the number of high-effort options performed by participants (models 1 and 3) and the mental effort perception, extracted with the behavioral model (model 2) using a selected set of metabolite concentrations. We used the *XGBRegressor* function from the Python *XGBoost* package to fit both models. XGBoost includes several adjustable hyperparameters. We optimized the step size shrinkage (eta), maximum depth of the tree (max_depth), minimum sum of instance weight (min_child_weight), and regularization parameters (gamma, lambda, alpha) through Bayesian optimization with the *hyperopt* Python package and CVLOO [48]. We assessed our model's prediction performance by correlating the predicted and true values of the target variables in a holdout sample that was not utilized in the model learning process. The train and test datasets were loaded into data frames using the *pandas* Python package and evaluated using model assessment metrics computed with the *numpy* Python package. Additionally, we computed the SHAP values using the *shap* Python package [49].

Results

Our study was designed to explore how inter-individual variation in 7T ^{1}H-MRS measured metabolites in the dmPFC/dACC (see **Fig. 1a,c**) can predict differences in physical and mental motivated behavior (**Fig. 1d-e**) across individuals. Additionally, we performed ^{1}H-MRS scans in the AI to assess the specificity of our predictive findings (**Fig. 1b**). Out of 75 participants recruited, data from 69 were fully valid for analyses (36 females; average age: 30 ± 4; BMI: 23.1 ± 3.2). To minimize any external

influences on the metabolic state of our participants, we included only individuals aged 25 to 40 years. We consistently started the experiments at 2 PM and asked participants to avoid eating at least 1h before the experiment to minimize the potential effects of hunger, digestion, and circadian rhythms on our metabolic measurements. Participants also had to avoid from performing any intense physical activity the day of the experiment and the preceding day.

Behavioral task

To assess motivated behavior, participants performed a behavioral task comprising 216 trials in 4 blocks. To ensure task feasibility and prevent participants from perceiving decisions as risky which could bias the effort perception [50], we calibrated the task individually during the training period (**Fig. 1**). In every trial, participants were presented with a choice between two options, characterized by differing monetary incentives and levels of required effort (**Fig. 1d-e**). These comprised a fixed low-effort option and a second option, where the effort level varied among three predefined levels. After making their choice, participants were required to perform the task at the selected effort level. This step was crucial to ensure that their decisions accurately reflected the presented effort levels. Notably, participants successfully completed the chosen effort in 95 ± 3.7% (mean ± SD) of the trials involving mental effort, and in 98 ± 3.4% of those requiring physical effort. Increased effort difficulty, associated with the high-effort option, resulted in fewer selections of high-effort/high-reward incentives in both physical and mental tasks **(Fig. S2a,d**), indicative of effort aversion. Effort aversion can be explained by the fact that, in our task, selecting higher difficulty levels led to tangible consequences: in the physical task, choosing the more effortful option correlated with higher handgrip force production (**Fig. S2b-c**). In the mental task, it resulted in a higher number of errors that seemed compensated by an elevated cognitive efficiency, defined as the ratio between the number of correct answers divided by time (**Fig. S2e-f**). In other words, these outcomes corroborate the task's effectiveness in quantifying motivational dynamics for both types of effort.

Importantly, the proportion of high mental effort choices and high physical effort choices were not correlated to one another ($r = 0.22$, $p = 0.06$).

dmPFC/dACC metabolites explain motivated behavior

To determine if dmPFC/dACC metabolite levels can predict the proportion of high mental effort (HME) and high physical effort (HPE) effort choices made by participants, we employed a gradient tree boosting regression model with metabolite concentrations as regressors. Our feature selection process, applied to 18 features including metabolites and standard ratios (detailed in Supplementary Materials), identified 8 features relevant for HME and 4 for HPE prediction (**Fig. 2**). To enhance data robustness and minimize overfitting, we adopted a train/validation/test approach with cross-

validation leave-one-out (CVLOO) design, splitting data into training/validation and testing sets with an 80% ratio, resulting in training/validation (N = 55) and testing (N = 14) datasets. We trained extreme gradient boosting trees (XGBoost) to fit linear response functions to HME and HPE, utilizing Bayesian optimization for hyperparameter tuning. The prediction error of the model was quantified using the root mean square error (RMSE).

For HPE, the model showed a medium fit in training and validation (train RMSE = 0.16%, validation RMSE = 16.06%), and a non-significant result on the test set (test RMSE = 23.00%, r = 0.015, p = 0.47), explaining only 5% of the variance (**Fig. 2a**). A permutation test with 5000 permutations further indicated that these results were not above chance level (95th percentile = 17.38 > model RMSE = 23.00) (**Fig. 2b**), indicating that HPE could not be significantly predicted with the combinations of baseline dmPFC/dACC metabolites available in our dataset. Similarly, training a model on metabolites from the AI, resulted in poor and non-significant performance (test RMSE = 24.46%, r = 0.24, p = 0.4), leading us to discard HPE prediction from further analysis.

In contrast, for HME, the model demonstrated a good fit (train RMSE = 0.05%, validation RMSE = 13.05%) and a consistent result in the unbiased estimate that is the test set (test RMSE = 12.51%, r = 0.49, p = 0.034), explaining 25% of the variance (**Fig. 2c**). The permutation test with 5000 permutations confirmed that our model's predictions significantly exceeded chance level (95th percentile = 13.48 > model RMSE = 12.51) (**Fig. 2d**). These results support our hypothesis that dmPFC/dACC metabolite concentrations can predict inter-individual variation in motivated behavior, specifically demonstrating their predictive power in the context of mental effort tasks.

To understand the impact of individual metabolites in the XGBoost model for predicting HME, we analyzed the Shapley Additive exPlanations (SHAP) values. The identified features included in descending order of their importance (determined by the magnitude of each feature's SHAP value) are glutamate (Glu), lactate (Lac), glutamine (Gln), Glutamine + Glutamate (Glx), N-acetylaspartate (NAA), phosphocreatine + creatine (PCr + Cr), aspartate (Asp) and glutathione (GSH) (**Fig. 2e**). Thus, glutamate and lactate emerged as the top discriminating features.

Importantly, our SHAP analysis of the data distribution for each predictive feature/metabolite revealed that specific metabolite concentrations do not have a linear relationship with HME. Indeed, neither glutamate (r = -0.19, p = 0.12) nor lactate (r = -0.13, p = 0.27) showed a linear relationship with HME. Particularly for glutamate, extreme values – either low or high – were negatively associated with HME, indicating a non-linear relationship. Employing Bayesian model comparison to determine the best model linking glutamate with HME, the most accurate fit featured an inverted U-shape relation, based on the mean-centered squared score of glutamate concentrations (r = 0.36, p = 0.003), as

supported by both the Akaike Information Criterion (AIC) and Bayesian Information Criterion (BIC) (**Fig. S3**). However, no pattern was observed for lactate's relationship with HME, supporting that its contribution lies in the multivariate model.

To determine if the metabolites relevant for HME are specific to the dmPFC/dACC region, we similarly assessed the ability of AI metabolite concentrations to predict HME. We applied the same model training process used for the dmPFC/dACC to AI metabolite concentrations. However, this AI-based model did not achieve statistical significance in predicting HME in our test set ($r = -0.4$, $p = 0.92$) (**Fig. 2f**), nor in the permutation test (95th percentile = 13.81% > model RMSE = 17.88%) (**Fig. 2g**).

Computational modeling of motivated behavior

Thus far, our analysis has shown the capability of dmPFC/dACC metabolites to predict HME using XGBoost. However, since motivation, and by extension HME, is a complex construct composed of multiple elements like reward sensitivity or effort aversion among many others [1,2,44], the specific behavioral components related to metabolism in this brain region remain to be elucidated. We designed our task and a computational model in order to disentangle the different behavioral parameters that could influence HME in our task. These behavioral parameters are the sensitivities to reward (kR) or punishment (kP), to physical (kEp) or mental (kEm) effort, and the impact of physical fatigue (kFp) or mental learning progress over time (kLm), along with a general bias to select the high effort options (bias). Computational methods help deepening our understanding of behavioral mechanisms and uncovering neurobiological correlates otherwise not observable [2,51,52]. Following best practices in computational modeling [53], we first verified whether our behavioral parameters were recoverable using simulations (**Fig. 3a**) and then confirmed that parameters were not confounded with each other (**Fig. 3b**). Parameter recovery, assessed by comparing simulation parameters with those optimized, was successful in average more than 78% of simulations for all the parameters, except for kLm which was recovered in 44% of simulations, a still rather reasonable result (**Fig. 3a**). No spurious correlations ($-0.5 < r < 0.5$) were detected between parameters (**Fig. 3b**), allowing for independent and sensitive recovery of each of the seven parameters (Palminteri et al., 2017). Thus, our model recovered each of the seven parameters independently and sensitively.

Further validation was performed by challenging our behavioral model against variants with fewer parameters (**Fig. S3**). Model comparisons unanimously highlighted the importance of all the extracted parameters (i.e., kR, kP, kEm, kEp, kLm, kFp, bias) in describing participants' behavior, despite the penalization for the added complexity of each additional parameter in the comparison process. Importantly, our model closely mirrored participant choices (median absolute error of 20.03 ± 7%,

goodness-of-fit $R^2 = 0.46$) (**Fig. 3c-d**), effectively capturing the tendency of participants to choose more effortful options when monetary incentives were higher or the associated effort was less demanding.

dmPFC/dACC metabolites specifically explain sensitivity to mental effort

Next, we sought to determine whether dmPFC/dACC metabolites could explain any of the five idiosyncratic parameters characterizing HME modeling from the computational modeling above. Given that cognitive effort is often perceived as aversive, which influences action avoidance [55], we initially focused on sensitivity to mental effort (kEm) from metabolite concentrations. The dataset was split into 75% for training/validation (N=53) and 25% for testing (N = 18), with hyperparameter tuning conducted using *hyperopt* and CVLOO. The XGBoost regression model showed a good level of accuracy in predicting kEm (range = 2.13, train RMSE = 0.34, validation RMSE = 0.75), and the test set yielded a modest prediction error (test RMSE = 0.64, $r = 0.4$, $p = 0.046$) (**Fig. 4a**), accounting for 16% of kEm's variance. This was confirmed by a permutation test, which indicated predictions significantly above chance level (95th percentile = 0.73 > model RMSE = 0.64) **(Fig. 4b**). In contrast, training a model to predict other parameters involved in mental-effort decision making such as reward sensitivity (kR), punishment sensitivity (kP), mental learning progress (kLm), and bias resulted in no significant predictions (all $p > 0.4$). This further reinforces the fact that our model better predicts cognitive effort sensitivity and choices.

SHAP values on the impact of the four metabolites predicting kEm prediction (**Fig. 4c**) highlighted glutathione (GSH), lactate and aspartate as the most discriminating features. Whereas no linear pattern was observed for GSH or lactate, aspartate exhibited a positive linear correlation with kEm ($r = 0.42$, $p < 0.001$) (**Fig. S4b**).

Refining the model explaining mental effort decision-making with essential biomarkers

Thus, we have found two effective XGBoost models for HME and kEm, utilizing 8 and 4 dmPFC/dACC metabolites, respectively. We next applied a parsimonious approach to determine if a smaller subset of metabolites could predict HME, aiming to balance simplicity with explanatory power [56]. This approach aligns with cognitive neuroscience and machine learning practices, where effective models prioritize high predictive accuracy with minimal parameters [57]. However, selecting the top two (i.e., glutamate and lactate; **Fig. S5a-c**) or top three (i.e., glutamate, lactate, and glutamine; **Fig. S5d-f**) predictors from our SHAP analysis failed to yield a significant prediction.

Inspired by efforts to integrate biological context in machine learning for improved relevance and interpretability [58], we examined metabolic overlap among the top-ranked metabolites. While aspartate ranked highly in the kEm model, it was lower in the HME model, possibly due to its biosynthetic relationship with glutamate and glutamine in the TCA cycle (**Fig. 5**) [59]. Machine

learning's tendency to minimize correlated features might have undervalued aspartate's role. Significant intercorrelations among these metabolites (**Fig. S4g**) support this hypothesis, suggesting aspartate may provide unique predictive information despite its lower ranking. In contrast, lactate, uncorrelated with glutamate ($r = 0.03$, $p = 0.77$) or aspartate ($r = 0.19$, $p = 0.11$), retained distinct variance. This prompted re-evaluation of glutamate, aspartate, and lactate concentrations in the dmPFC/dACC for predicting HME and their role as biomarkers for mental effort decision-making.

We retrained an XGBoost model using a train/validation/test analysis design with a CVLOO approach. Data were split into training/validation (80%, N = 55) and testing (20%, N = 14) sets. XGBoost with RMSE as the error metric, achieved a good fit on the training (RMSE = 0.75%) and validation (RMSE = 15.68%) sets. (**Fig. 6a,b**) and performed well on the test set (RMSE = 12.56%, $r = 0.64$, $p = 0.0063$), explaining 41% of the variance (**Fig. 6c**). A permutation test (5000 permutations) confirmed predictions significantly exceeded chance levels (95th percentile = 13.59 > model RMSE = 12.56). These results indicate that a machine learning model based on a few dmPFC/dACC metabolite concentrations can predict participants' willingness to exert mental effort.

SHAP analysis revealed complex relationships. Glutamate and lactate showed no linear correlations with HME (glutamate: $r = -0.19$, $p = 0.12$; lactate: $r = -0.13$, $p = 0.27$), though extreme glutamate values suggested a quadratic relationship (**Fig. S6**). Aspartate displayed a strong negative linear correlation with HME ($r = -0.37$, $p = 0.002$) (**Fig. S4a**).

Plasma and brain metabolite concentrations

To investigate relationships between plasma and brain metabolite concentrations, we examined correlations between plasma levels of glutamate, aspartate, and lactate and their counterparts in the dmPFC/dACC (**Fig. S7**). Given glutamate's lower plasma concentration than its precursor glutamine [60], we also analyzed glutamine concentrations. Similar analyses were performed for the AI as a comparison region. No significant correlations were found between plasma and dmPFC/dACC or AI concentrations of glutamate and aspartate. Lactate showed region-specific correlations, being significant in the dmPFC/dACC ($r = 0.27$, $p = 0.023$) but not in the AI ($r = 0.14$, $p = 0.36$). Conversely, glutamine exhibited a strong positive association in both regions ($r = 0.54$, $p = 1.5 \cdot 10^{-5}$ in dmPFC/dACC; $r = 0.34$, $p = 0.014$ in AI), suggesting a broader brain-plasma relationship.

Discussion

Differences in individuals' willingness to undertake incentivized effortful tasks can profoundly influence their life trajectories [3–5,61]. The dmPFC/dACC and the AI, both part of the salience network [65–68], have been implicated in effort-based decision-making [2,8,9,11,12,14,62], but the

specific neurobiological factors driving individual variability in this domain remain unclear. Our study bridges this knowledge gap by identifying key neurometabolic predictors in the dmPFC/dACC that account for variability in mental effort exertion.

Departing from earlier studies that focused primarily on individual metabolites [32,34,40,41,63,64], our multivariate approach identified a broader view of the neurometabolic processes associated with mental effort-based decision-making. Using high-field (7T) ^{1}H-MRS and machine learning, our initial models identified several metabolites in the dmPFC/dACC as relevant to predicting both high mental effort exertion (HME) and sensitivity to mental effort (kEm). Subsequent refinement of these models revealed that a smaller subset of key metabolites (glutamate, lactate, and aspartate) in the dmPFC/dACC emerged as the most robust predictors of mental effort motivation. Specifically, aspartate and lactate levels correlated positively with aversion to mental effort, while glutamate exhibited an inverted-U shape relationship with HME, suggesting its optimal contribution lies within a specific, moderate concentration range. These results emphasize the complex, nonlinear interactions between neurometabolic markers and mental effort motivation, with the refined model explaining up to 40% of HME variance. Importantly, models using AI metabolites or predicting HPE were inconclusive, supporting a particularly predictive value of dmPFC/dACC metabolites in mental effort-based decision-making.

Glutamate, aspartate, and lactate are central to brain metabolism, playing crucial roles in supporting physiological functions critical for cognitive processes [38,39,69]. These metabolites, interconnected through the tricarboxylic acid (TCA) cycle and glycolysis, underpin neuronal energy supply, neurotransmission, and amino acid synthesis [70,73,74]. Their combined predictive role for HME suggests that their interplay within the dmPFC/dACC may fine-tune neural computations related to mental effort feasibility and desirability. In addition, the SHAP analysis also identified the importance of other metabolites, such as glutathione related to antioxidant pathways, and glutamine, to a lesser extent. Previous research showed a positive involvement of glutathione in the nucleus accumbens on the regulation of physical effort exertion [35], while glutamine levels in the nucleus accumbens were negatively related to physical effort perception [32]. These findings suggest that metabolic pathways impacting motivated behavior may vary across different brain areas.

Specifically, the neurometabolic profile in the dmPFC/dACC predictive of low motivation for mental effort, involving combinations of elevated levels of glutamate, aspartate, and lactate, suggests a metabolic imbalance potentially indicative of mitochondrial malfunction [75–77]. Such dysfunction could signal a disruption in the TCA cycle, as suggested by elevated aspartate and glutamate levels [78], and a compensatory shift towards glycolysis due to impaired oxidative phosphorylation,

indicated by increased lactate levels. These disturbances may impair ATP production, amino acids, nucleotides, and bioactive molecules synthesis, essential for neuronal function and integrity [26,27], as well as neurotransmitter synthesis and signaling pathways [79]. Rodent models suggest that mitochondrial dysfunction impairs performance in demanding behavioral tasks [26,80,81], and similar metabolic imbalances within the dmPFC/dACC may affect energy-intensive cognitive processes, diminishing both motivation and cognitive control mechanisms.

Inspecting the weights of the metabolites within the model provides further insights into their potential contributions, particularly through the observed quadratic association of glutamate with mental effort choices and the strong negative linear correlation of aspartate with high mental effort (HME) choices. Consistent with evidence that both low and high glutamate concentrations can impair cellular functions [82] and contribute to cognitive deficits [83,84], our study highlights that dmPFC/dACC glutamate levels are optimal for cognitive effort motivation only within an optimal range. Aspartate's negative association with HME choices and its link to reduced cognitive efficiency during effortful tasks highlight its significant, yet rather underappreciated role in cognitive metabolism and neuronal activity. Lactate's contribution to HME and mental effort sensitivity (kEm) becomes evident in the multivariate context, with elevated levels potentially reducing HME choices through mechanisms that extend beyond its traditional role as an energy substrate [85]. Brain lactate levels increase following systemic physiological changes, such as intense exercise [86,87], and elevated lactate is associated with pathologies like schizophrenia and depression [88–91], which include motivational deficits as core symptoms [61].

Notably, while metabolite levels in the brain, exhibit remarkable stability over time [92–94], indicating distinct neuro-metabolic phenotypes [95], they remain susceptible to changes. For example, stress can dynamically alter glutamate levels in the prefrontal cortex [96,97], thereby influencing decision-making [98,99]. This highlights potential intervention targets for conditions characterized by motivational deficits. Our findings further indicate that brain concentrations of glutamate and aspartate are largely independent of their plasma levels, consistent with prior evidence showing minimal contribution of plasma glutamate to brain levels [60]. In contrast, the observed positive correlation between plasma and dmPFC/dACC lactate concentrations aligns with the unique transport dynamics of lactate across the blood-brain barrier [100]. While the possibility of impacting brain concentrations of glutamate and aspartate through peripheral interventions appears limited, the plasma-brain lactate correlation suggests that systemic changes could impact brain metabolism and motivated behavior. Accordingly, interventions such as exercise or direct lactate administration may modulate brain lactate levels, influencing motivated behavior and cognitive engagement.

While our study presents significant insights, it also has certain limitations. Although the models developed for HME and kEm yielded significant and robust predictions, they were trained on a relatively small sample size. However, the recruitment and testing of 75 subjects in the demanding 7T experimental studies represent a considerable sample size for this field. Future research should benchmark the predictive capacity of these models and evaluate their generalizability to new datasets and other mental effort paradigms.

In conclusion, our study advances the understanding of neurometabolism in cognitive neuroscience, particularly in relation to motivated behavior. By identifying the combined predictive roles of glutamate, lactate and aspartate in the dmPFC/dACC, we highlight their collective ability to predict mental effort in healthy individuals. This work bridges the gap between metabolic processes and cognitive function and introduces a novel approach to assess the collective impact of multiple metabolites. Our findings provide a foundation for future investigations, including causal analyses in animal models, and position a subset of dmPFC/dACC metabolites as biological biomarkers for mental effort and motivation.

Acknowledgments

We thank the nursing staff at EPFL-Point Santé (Viviane Depuydt-Linder and Chiyama Mathivathanasekaram) and Centre Medical des Arcades (Lausanne), as well as members of the EPFL-LGC laboratory for their support in blood collection and processing. We thank Antonius Wiehler, Alizée Lopez-Persem and Bogdan Draganski for their inputs to the behavioral experimental design, and Olivier Ciclet (Nestlé Research), Adrien Frezal (Nestlé Research), and Irina Monnard (Nestlé Research) for their contributions to the plasma analyses.

Funding

Swiss National Science Foundation grant 10531C_ 212914 (CS)

Swiss National Science Foundation grant CRSII5_183564 (CS)

Novartis Foundation for Medical-Biological Research grant 21B110 (NC)

Foundation for the Encouragement of Nutrition Research in Switzerland (SFEFS) grant 607 (NC)

European Union's Horizon 2020 Research and Innovation Program (Marie Sklodowska-Curie) grant 101032219 (NC)

Intramural funding from the EFPL (C.S.)

Conflict of interest

JPG and BC are employees of Société des Produits Nestlé SA. C.S. is a member of the scientific advisory board of Amazentis/Timeline S.A and consults for Vandria S.A.

References

1. Chong TT-J, Bonnelle V, Husain M. Quantifying motivation with effort-based decision-making paradigms in health and disease. Prog. Brain Res., vol. 229, Elsevier; 2016. p. 71–100.
2. Pessiglione M, Vinckier F, Bouret S, Daunizeau J, Le Bouc R. Why not try harder? Computational approach to motivation deficits in neuro-psychiatric diseases. Brain. 2018;141:629–650.
3. Duckworth AL, Eichstaedt JC, Ungar LH. The Mechanics of Human Achievement: Newtonian Model of Achievement. Soc Personal Psychol Compass. 2015;9:359–369.
4. Epstein J, Silbersweig D. The Neuropsychiatric Spectrum of Motivational Disorders. J Neuropsychiatry Clin Neurosci. 2015;27:7–18.
5. Kanfer R, Frese M, Johnson RE. Motivation related to work: A century of progress. J Appl Psychol. 2017;102:338–355.
6. Le Heron C, Apps. MAJ, Husain M. The anatomy of apathy: A neurocognitive framework for amotivated behaviour. Neuropsychologia. 2018;118:54–67.
7. Bartra O, McGuire JT, Kable JW. The valuation system: A coordinate-based meta-analysis of BOLD fMRI experiments examining neural correlates of subjective value. NeuroImage. 2013;76:412–427.
8. Clairis N, Lopez-Persem A. Debates on the dorsomedial prefrontal/dorsal anterior cingulate cortex: insights for future research. Brain. 2023:awad263.
9. Lopez-Gamundi P, Yao Y-W, Chong TT-J, Heekeren HR, Mas-Herrero E, Marco-Pallarés J. The neural basis of effort valuation: A meta-analysis of functional magnetic resonance imaging studies. Neurosci Biobehav Rev. 2021;131:1275–1287.
10. Soutschek A, Nadporozhskaia L, Christian P. Brain stimulation over dorsomedial prefrontal cortex modulates effort-based decision making. Cogn Affect Behav Neurosci. 2022;22:1264–1274.
11. Chong TT-J, Apps M, Giehl K, Sillence A, Grima LL, Husain M. Neurocomputational mechanisms underlying subjective valuation of effort costs. PLOS Biol. 2017;15:e1002598.
12. Kurniawan IT, Grueschow M, Ruff CC. Anticipatory Energization Revealed by Pupil and Brain Activity Guides Human Effort-Based Decision Making. J Neurosci. 2021;41:6328–6342.
13. Clairis N, Pessiglione M. Value Estimation versus Effort Mobilization: A General Dissociation between Ventromedial and Dorsomedial Prefrontal Cortex. J Neurosci. 2024;44.
14. Le Bouc R, Borderies N, Carle G, Robriquet C, Vinckier F, Daunizeau J, et al. Effort avoidance as a core mechanism of apathy in frontotemporal dementia. Brain. 2023;146:712–726.
15. Darby RR, Joutsa J, Burke MJ, Fox MD. Lesion network localization of free will. Proc Natl Acad Sci. 2018;115:10792–10797.
16. Morella IM, Brambilla R, Morè L. Emerging roles of brain metabolism in cognitive impairment and neuropsychiatric disorders. Neurosci Biobehav Rev. 2022;142:104892.
17. Ülgen DH, Ruigrok SR, Sandi C. Powering the social brain: Mitochondria in social behaviour. Curr Opin Neurobiol. 2023;79:102675.
18. Yellen G. Fueling thought: Management of glycolysis and oxidative phosphorylation in neuronal metabolism. J Cell Biol. 2018;217:2235–2246.
19. Gailliot MT, Baumeister RF. The Physiology of Willpower: Linking Blood Glucose to Self-Control. Personal Soc Psychol Rev. 2007;11:303–327.
20. Gailliot MT, Baumeister RF, DeWall CN, Maner JK, Plant EA, Tice DM, et al. Self-control relies on glucose as a limited energy source: willpower is more than a metaphor. J Pers Soc Psychol. 2007;92:325–336.
21. Dang J. Testing the role of glucose in self-control: A meta-analysis. Appetite. 2016;107:222–230.
22. Job V, Walton GM, Bernecker K, Dweck CS. Beliefs about willpower determine the impact of glucose on self-control. Proc Natl Acad Sci. 2013;110:14837–14842.

23. Lange F, Eggert F. Sweet delusion. Glucose drinks fail to counteract ego depletion. Appetite. 2014;75:54–63.
24. Vadillo MA, Gold N, Osman M. The Bitter Truth About Sugar and Willpower: The Limited Evidential Value of the Glucose Model of Ego Depletion. Psychol Sci. 2016;27:1207–1214.
25. Devine MJ, Kittler JT. Mitochondria at the neuronal presynapse in health and disease. Nat Rev Neurosci. 2018;19:63–80.
26. Gebara E, Zanoletti O, Ghosal S, Grosse J, Schneider BL, Knott G, et al. Mitofusin-2 in the Nucleus Accumbens Regulates Anxiety and Depression-like Behaviors Through Mitochondrial and Neuronal Actions. Biol Psychiatry. 2021;89:1033–1044.
27. Ghosal S, Gebara E, Ramos-Fernández E, Chioino A, Grosse J, Guillot De Suduiraut I, et al. Mitofusin-2 in nucleus accumbens D2-MSNs regulates social dominance and neuronal function. Cell Rep. 2023;42:112776.
28. Lutas A, Yellen G. The ketogenic diet: metabolic influences on brain excitability and epilepsy. Trends Neurosci. 2013;36:32–40.
29. Morató L, Astori S, Zalachoras I, Rodrigues J, Ghosal S, Huang W, et al. eNAMPT actions through nucleus accumbens NAD^+/SIRT1 link increased adiposity with sociability deficits programmed by peripuberty stress. Sci Adv. 2022;8:eabj9109.
30. Cherix A, Larrieu T, Grosse J, Rodrigues J, McEwen B, Nasca C, et al. Metabolic signature in nucleus accumbens for anti-depressant-like effects of acetyl-L-carnitine. eLife. 2020;9:e50631.
31. Lapidus KAB, Gabbay V, Mao X, Johnson A, Murrough JW, Mathew SJ, et al. In vivo 1H MRS study of potential associations between glutathione, oxidative stress and anhedonia in major depressive disorder. Neurosci Lett. 2014;569:74–79.
32. Strasser A, Luksys G, Xin L, Pessiglione M, Gruetter R, Sandi C. Glutamine-to-glutamate ratio in the nucleus accumbens predicts effort-based motivated performance in humans. Neuropsychopharmacology. 2020;45:2048–2057.
33. Wang AM, Pradhan S, Coughlin JM, Trivedi A, DuBois SL, Crawford JL, et al. Assessing Brain Metabolism With 7-T Proton Magnetic Resonance Spectroscopy in Patients With First-Episode Psychosis. JAMA Psychiatry. 2019;76:314.
34. Wiehler A, Branzoli F, Adanyeguh I, Mochel F, Pessiglione M. A neuro-metabolic account of why daylong cognitive work alters the control of economic decisions. Curr Biol. 2022;32:3564-3575.e5.
35. Zalachoras I, Ramos-Fernández E, Hollis F, Trovo L, Rodrigues J, Strasser A, et al. Glutathione in the nucleus accumbens regulates motivation to exert reward-incentivized effort. eLife. 2022;11:e77791.
36. Clairis N, Barakat A, Brochard J, Xin L, Sandi C. A neurometabolic mechanism involving dmPFC/dACC lactate in physical effort-based decision-making. Mol Psychiatry. 2024:1–15.
37. Maddock RJ, Buonocore MH. MR spectroscopic studies of the brain in psychiatric disorders. Curr Top Behav Neurosci. 2012;11:199–251.
38. Rae CD. A guide to the metabolic pathways and function of metabolites observed in human brain 1H magnetic resonance spectra. Neurochem Res. 2014;39:1–36.
39. Rae CD, Baur JA, Borges K, Dienel G, Díaz-García CM, Douglass SR, et al. Brain energy metabolism: A roadmap for future research. J Neurochem. 2024:jnc.16032.
40. Jocham G, Hunt LT, Near J, Behrens TEJ. A mechanism for value-guided choice based on the excitation-inhibition balance in prefrontal cortex. Nat Neurosci. 2012;15:960–961.
41. Yoon JH, Grandelis A, Maddock RJ. Dorsolateral Prefrontal Cortex GABA Concentration in Humans Predicts Working Memory Load Processing Capacity. J Neurosci. 2016;36:11788–11794.
42. Aben B, Buc Calderon C, Van den Bussche E, Verguts T. Cognitive Effort Modulates Connectivity between Dorsal Anterior Cingulate Cortex and Task-Relevant Cortical Areas. J Neurosci Off J Soc Neurosci. 2020;40:3838–3848.

43. Seeley WW. The Salience Network: A Neural System for Perceiving and Responding to Homeostatic Demands. J Neurosci Off J Soc Neurosci. 2019;39:9878–9882.
44. Bonnelle V, Veromann K-R, Burnett Heyes S, Lo Sterzo E, Manohar S, Husain M. Characterization of reward and effort mechanisms in apathy. J Physiol-Paris. 2015;109:16–26.
45. Westbrook A, van den Bosch R, Määttä JI, Hofmans L, Papadopetraki D, Cools R, et al. Dopamine Promotes Cognitive Effort by Biasing the Benefits Versus Costs of Cognitive Work. Neuroscience; 2019.
46. Daunizeau J, Adam V, Rigoux L. VBA: A Probabilistic Treatment of Nonlinear Models for Neurobiological and Behavioural Data. PLoS Comput Biol. 2014;10:e1003441.
47. Bicego M, Baldo S. Properties of the Box–Cox transformation for pattern classification. Neurocomputing. 2016;218:390–400.
48. Bergstra J, Yamins D, Cox DD. Making a Science of Model Search: Hyperparameter Optimization in Hundreds of Dimensions for Vision Architectures. 2013. 2013.
49. Lundberg SM, Erion GG, Lee S-I. Consistent Individualized Feature Attribution for Tree Ensembles. 2019.
50. Lopez-Gamundi P, Mas-Herrero E, Marco-Pallares J. Disentangling effort from probability of success: Temporal dynamics of frontal midline theta in effort-based reward processing. Cortex. 2024;176:94–112.
51. Nassar MR, Frank MJ. Taming the beast: extracting generalizable knowledge from computational models of cognition. Curr Opin Behav Sci. 2016;11:49–54.
52. Corrado G, Doya K. Understanding Neural Coding through the Model-Based Analysis of Decision Making. J Neurosci. 2007;27:8178–8180.
53. Wilson RC, Collins AG. Ten simple rules for the computational modeling of behavioral data. eLife. 2019;8:e49547.
54. Palminteri S, Wyart V, Koechlin E. The Importance of Falsification in Computational Cognitive Modeling. Trends Cogn Sci. 2017;21:425–433.
55. Vogel TA, Savelson ZM, Otto AR, Roy M. Forced choices reveal a trade-off between cognitive effort and physical pain. eLife. 2020;9:e59410.
56. Vandekerckhove J, Matke D, Wagenmakers E-J. Model Comparison and the Principle of Parsimony. Oxf. Handb. Comput. Math. Psychol., vol. 300, 2015.
57. Takahashi Y, Ueki M, Yamada M, Tamiya G, Motoike IN, Saigusa D, et al. Improved metabolomic data-based prediction of depressive symptoms using nonlinear machine learning with feature selection. Transl Psychiatry. 2020;10:157.
58. Zampieri G, Vijayakumar S, Yaneske E, Angione C. Machine and deep learning meet genome-scale metabolic modeling. PLOS Comput Biol. 2019;15:e1007084.
59. Holten AT, Gundersen V. Glutamine as a precursor for transmitter glutamate, aspartate and GABA in the cerebellum: a role for phosphate-activated glutaminase. J Neurochem. 2008;104:1032–1042.
60. Smith QR. Transport of Glutamate and Other Amino Acids at the Blood-Brain Barrier. J Nutr. 2000;130:1016S-1022S.
61. Husain M, Roiser JP. Neuroscience of apathy and anhedonia: a transdiagnostic approach. Nat Rev Neurosci. 2018;19:470–484.
62. Shenhav A, Musslick S, Lieder F, Kool W, Griffiths TL, Cohen JD, et al. Toward a Rational and Mechanistic Account of Mental Effort. Annu Rev Neurosci. 2017;40:99–124.
63. Grachev ID, Kumar R, Ramachandran TS, Szeverenyi NM. Cognitive interference is associated with neuronal marker N-acetyl aspartate in the anterior cingulate cortex: an in vivo (1)H-MRS study of the Stroop Color-Word task. Mol Psychiatry. 2001;6:496, 529–539.
64. Yücel M, Harrison BJ, Wood SJ, Fornito A, Clarke K, Wellard RM, et al. State, trait and biochemical influences on human anterior cingulate function. NeuroImage. 2007;34:1766–1773.

65. Litt A, Plassmann H, Shiv B, Rangel A. Dissociating Valuation and Saliency Signals during Decision-Making. Cereb Cortex. 2011;21:95–102.
66. Seeley WW, Menon V, Schatzberg AF, Keller J, Glover GH, Kenna H, et al. Dissociable Intrinsic Connectivity Networks for Salience Processing and Executive Control. J Neurosci. 2007;27:2349–2356.
67. Uddin LQ. Salience processing and insular cortical function and dysfunction. Nat Rev Neurosci. 2015;16:55–61.
68. Uddin LQ, Yeo BTT, Spreng RN. Towards a Universal Taxonomy of Macro-scale Functional Human Brain Networks. Brain Topogr. 2019;32:926–942.
69. Li J, Xia Y, Xu H, Xiong R, Zhao Y, Li P, et al. Activation of brain lactate receptor GPR81 aggravates exercise-induced central fatigue. Am J Physiol-Regul Integr Comp Physiol. 2022;323:R822–R831.
70. Waagepetersen HS, Bakken IJ, Larsson OM, Sonnewald U, Schousboe A. Metabolism of Lactate in Cultured GABAergic Neurons Studied by ^{13}C Nuclear Magnetic Resonance Spectroscopy. J Cereb Blood Flow Metab. 1998;18:109–117.
71. McKenna MC, Sonnewald U, Huang X, Stevenson J, Zielke HR. Exogenous Glutamate Concentration Regulates the Metabolic Fate of Glutamate in Astrocytes. J Neurochem. 1996;66:386–393.
72. Schousboe A, Scafidi S, Bak LK, Waagepetersen HS, McKenna MC. Glutamate Metabolism in the Brain Focusing on Astrocytes. In: Parpura V, Schousboe A, Verkhratsky A, editors. Glutamate ATP Interface Metab. Signal. Brain, vol. 11, Cham: Springer International Publishing; 2014. p. 13–30.
73. Juaristi I, Contreras L, González-Sánchez P, Pérez-Liébana I, González-Moreno L, Pardo B, et al. The Response to Stimulation in Neurons and Astrocytes. Neurochem Res. 2019;44:2385–2391.
74. Pellerin L, Magistretti PJ. Sweet Sixteen for ANLS. J Cereb Blood Flow Metab. 2012;32:1152–1166.
75. Bianchi MC, Sgandurra G, Tosetti M, Battini R, Cioni G. Brain Magnetic Resonance in the Diagnostic Evaluation of Mitochondrial Encephalopathies. Biosci Rep. 2007;27:69–85.
76. Nunnari J, Suomalainen A. Mitochondria: In Sickness and in Health. Cell. 2012;148:1145–1159.
77. Schmiedel J, Jackson S, Schäfer J, Reichmann H. Mitochondrial Cytopathies. J Neurol. 2003;250:267–277.
78. Owen OE, Kalhan SC, Hanson RW. The Key Role of Anaplerosis and Cataplerosis for Citric Acid Cycle Function. J Biol Chem. 2002;277:30409–30412.
79. Magistretti PJ, Allaman I. A Cellular Perspective on Brain Energy Metabolism and Functional Imaging. Neuron. 2015;86:883–901.
80. Hollis F, Van Der Kooij MA, Zanoletti O, Lozano L, Cantó C, Sandi C. Mitochondrial function in the brain links anxiety with social subordination. Proc Natl Acad Sci. 2015;112:15486–15491.
81. van der Kooij MA, Hollis F, Lozano L, Zalachoras I, Abad S, Zanoletti O, et al. Diazepam actions in the VTA enhance social dominance and mitochondrial function in the nucleus accumbens by activation of dopamine D1 receptors. Mol Psychiatry. 2018;23:569–578.
82. Lau A, Tymianski M. Glutamate receptors, neurotoxicity and neurodegeneration. Pflüg Arch - Eur J Physiol. 2010;460:525–542.
83. Shirayama Y, Takahashi M, Osone F, Hara A, Okubo T. Myo-inositol, Glutamate, and Glutamine in the Prefrontal Cortex, Hippocampus, and Amygdala in Major Depression. Biol Psychiatry Cogn Neurosci Neuroimaging. 2017;2:196–204.
84. Nakahara T, Tsugawa S, Noda Y, Ueno F, Honda S, Kinjo M, et al. Glutamatergic and GABAergic metabolite levels in schizophrenia-spectrum disorders: a meta-analysis of 1H-magnetic resonance spectroscopy studies. Mol Psychiatry. 2022;27:744–757.
85. Magistretti PJ, Allaman I. Lactate in the brain: from metabolic end-product to signalling molecule. Nat Rev Neurosci. 2018;19:235–249.

86. Koush Y, Rothman DL, Behar KL, De Graaf RA, Hyder F. Human brain functional MRS reveals interplay of metabolites implicated in neurotransmission and neuroenergetics. J Cereb Blood Flow Metab. 2022;42:911–934.
87. Świątkiewicz M, Gaździński S, Madeyski M, Kossowski B, Langfort J, Bogorodzki P, et al. Increased brain 1H-MRS glutamate and lactate signals following maximal aerobic capacity exercise in young healthy males: an exploratory study. Biol Sport. 2023;40:665–673.
88. Ernst J, Hock A, Henning A, Seifritz E, Boeker H, Grimm S. Increased pregenual anterior cingulate glucose and lactate concentrations in major depressive disorder. Mol Psychiatry. 2017;22:113–119.
89. Machado-Vieira R, Zanetti MV, Otaduy MC, De Sousa RT, Soeiro-de-Souza MG, Costa AC, et al. Increased Brain Lactate During Depressive Episodes and Reversal Effects by Lithium Monotherapy in Drug-Naive Bipolar Disorder: A 3-T 1H-MRS Study. J Clin Psychopharmacol. 2017;37:40–45.
90. Rowland LM, Pradhan S, Korenic S, Wijtenburg SA, Hong LE, Edden RA, et al. Elevated brain lactate in schizophrenia: a 7 T magnetic resonance spectroscopy study. Transl Psychiatry. 2016;6:e967–e967.
91. Soeiro-de-Souza MG, Pastorello BF, Leite CDC, Henning A, Moreno RA, Garcia Otaduy MC. Dorsal Anterior Cingulate Lactate and Glutathione Levels in Euthymic Bipolar I Disorder: ^{1}H-MRS Study. Int J Neuropsychopharmacol. 2016;19:pyw032.
92. Lally N, An L, Banerjee D, Niciu MJ, Luckenbaugh DA, Richards EM, et al. Reliability of 7T ^{1}H-MRS measured human prefrontal cortex glutamate, glutamine, and glutathione signals using an adapted echo time optimized PRESS sequence: A between- and within-sessions investigation: 7T ^{1}H-MRS Glutamatergic Reliability. J Magn Reson Imaging. 2016;43:88–98.
93. Ross AJ, Sachdev PS, Wen W, Brodaty H. Longitudinal Changes During Aging Using Proton Magnetic Resonance Spectroscopy. J Gerontol A Biol Sci Med Sci. 2006;61:291–298.
94. Wang M-Y, Korbmacher M, Eikeland R, Craven AR, Specht K. The intra-individual reliability of 1 H-MRS measurement in the anterior cingulate cortex across 1 year. Hum Brain Mapp. 2024;45:e26531.
95. Wu B, Bagshaw AP, Hickey C, Kühn S, Wilson M. Evidence for distinct neuro-metabolic phenotypes in humans. NeuroImage. 2022;249:118902.
96. Sandi C. Glucocorticoids act on glutamatergic pathways to affect memory processes. Trends Neurosci. 2011;34:165–176.
97. Treccani G, Musazzi L, Perego C, Milanese M, Nava N, Bonifacino T, et al. Stress and corticosterone increase the readily releasable pool of glutamate vesicles in synaptic terminals of prefrontal and frontal cortex. Mol Psychiatry. 2014;19:433–443.
98. Sanacora G, Yan Z, Popoli M. The stressed synapse 2.0: pathophysiological mechanisms in stress-related neuropsychiatric disorders. Nat Rev Neurosci. 2022;23:86–103.
99. Sandi C. Stress and cognition. Wiley Interdiscip Rev Cogn Sci. 2013;4:245–261.
100. Hladky SB, Barrand MA. Fluid and ion transfer across the blood–brain and blood–cerebrospinal fluid barriers; a comparative account of mechanisms and roles. Fluids Barriers CNS. 2016;13:19.

Figure Legends

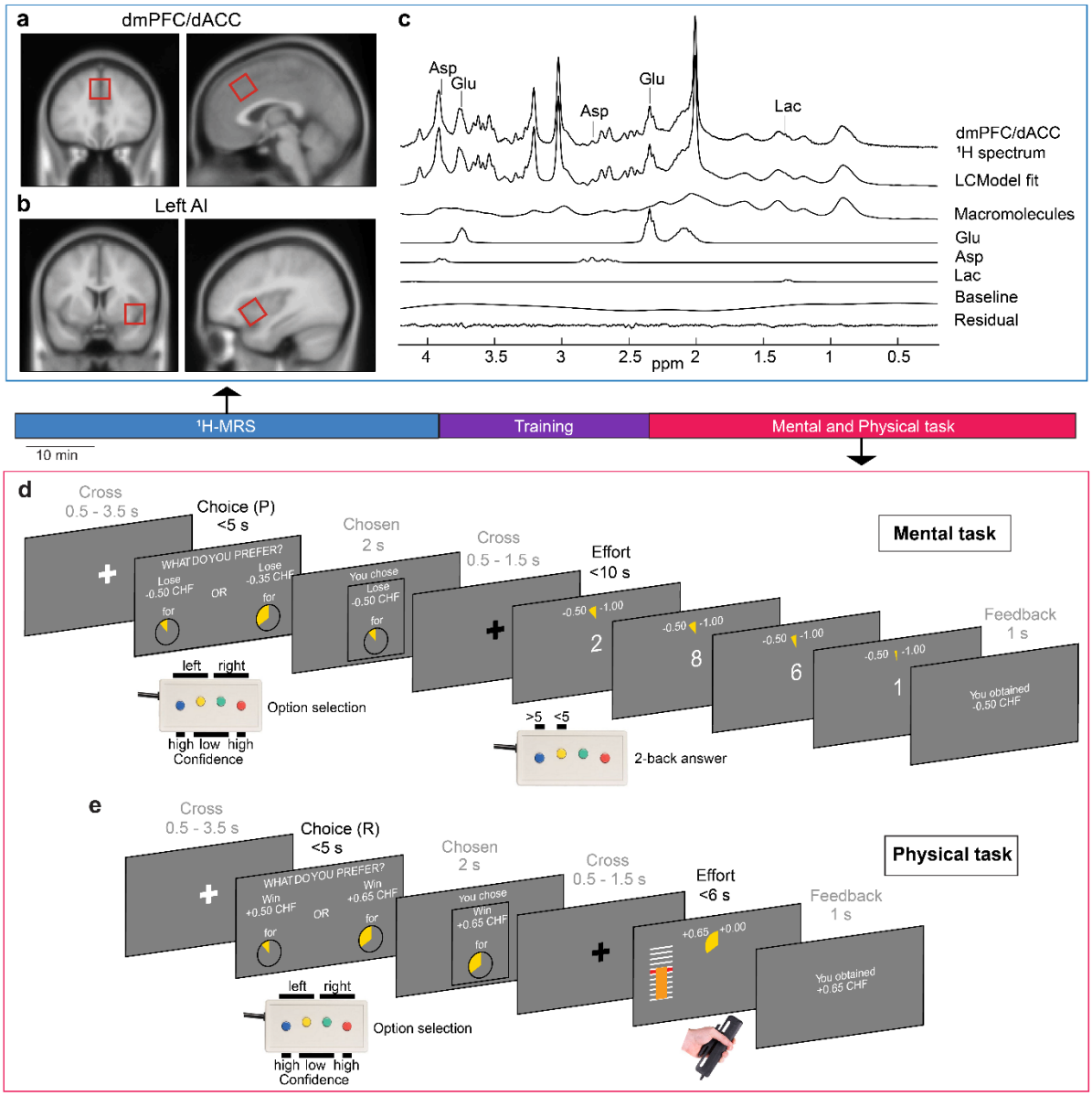

Fig. 1: Overview of experimental design. (**a-b**) Localization of dmPFC/dACC and AI voxels (20 x 20 x 20mm³) targeted for ¹H-MRS acquisitions. The voxels are displayed in coronal and sagittal sections, overlaid on the MNI152 T1 average anatomical scan for reference. (**c**) Example of a ¹H-MR spectrum obtained from the dmPFC/dACC. The spectrum showcases the LGCModel spectral fit, macromolecular signals, baseline, residual fit, and individual metabolite fits for glutamate (Glu), aspartate (Asp), and lactate (Lac). (**d-e**) Effort-based decision-making tasks. Participants choose between options varying in effort and monetary incentive (reward or punishment) levels, with the potential for higher effort leading to greater rewards or avoiding larger punishments. Each trial started with a fixation cross, followed by a 5-seconds window where participants had to pick up the option that looked the more interesting for them based on their subjective preferences. There was always one option associated to a low effort and a low monetary incentive, while the other was associated to a larger monetary incentive but also to a higher effort. Physical and mental efforts were segregated into distinct blocks (2 for each type of effort), while rewards and punishment incentives were intermixed across trials within each block. After the choice was made, the chosen option was briefly displayed, followed by another fixation cross with a jitter to separate decision-making from the effort phase. (**d**) In the mental

effort task, participants aimed to achieve a target number of correct responses within 10 seconds, determined by their prior calibration and the selected effort level. (**e**) In the physical effort task, participants had to maintain force above 55% of their maximal force for a duration depending on the chosen effort level (between 0.5 and 4.5s). Each trial ended with performance feedback indicating how much money was earned (or lost respectively) in the current trial.

High Physical Effort
dmPFC/dACC
metabolites

Testing set:
r = 0.015, p = 0.47

Permutation test:
True RMSE = 23.00%
95th percentile
RMSE = 17.38 %

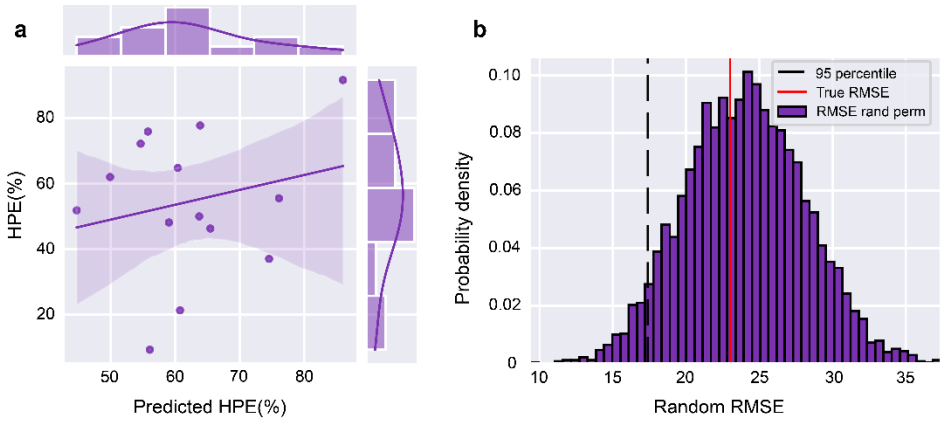

High Mental Effort
dmPFC/dACC
metabolites

Testing set:
r = 0.5, p = 0.034

Permutation test:
True RMSE = 12.51%
95th percentile
RMSE = 13.46 %

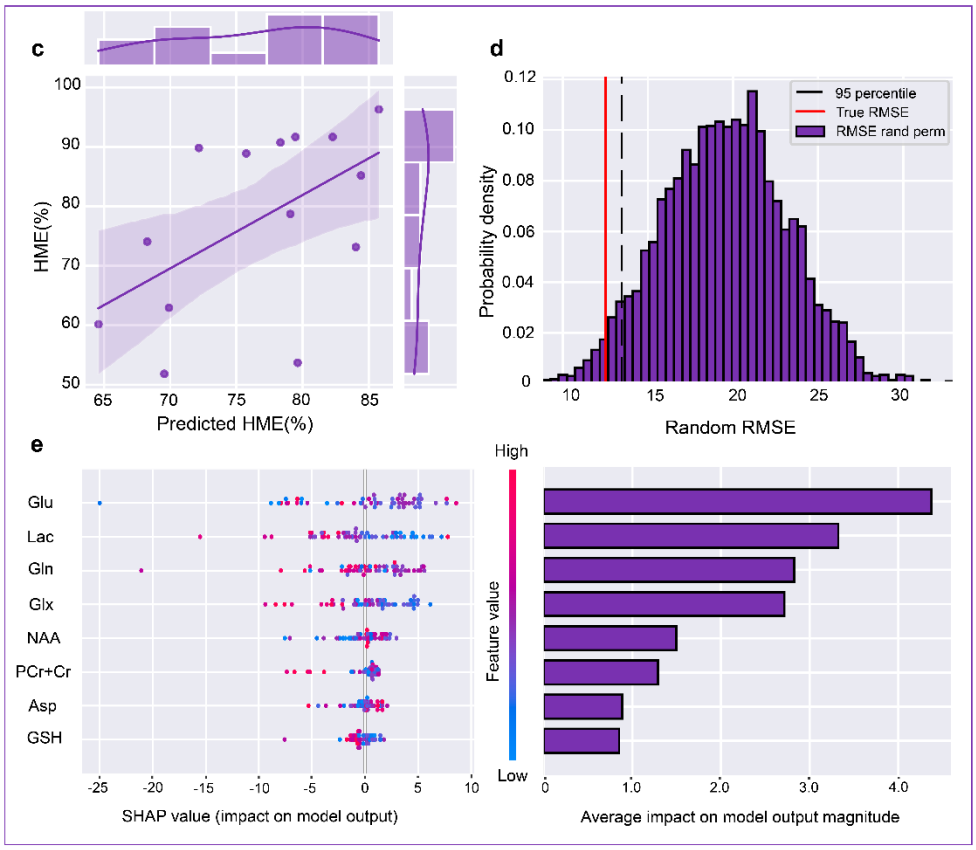

High Mental Effort
AI metabolites

Testing set:
r = -0.4, p = 0.92

Permutation test:
True RMSE = 17.88%
95th percentile
RMSE = 13.81 %

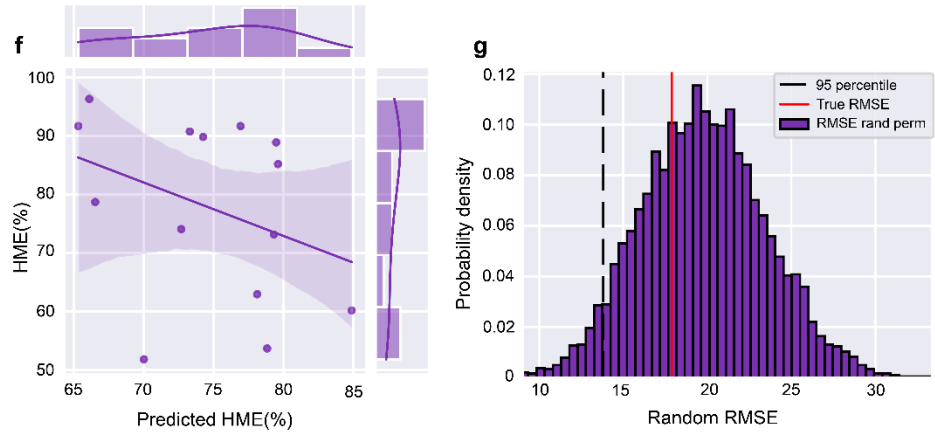

Fig. 2: Analysis of models' explanations for physical and mental effort choices based on metabolite concentrations in dmPFC/dACC and AI. (**a**) Analysis of high physical effort (HPE) explanations using dmPFC/dACC metabolite concentrations with an XGBoost model indicates a moderate correlation not reaching significance ($r = 0.015$, $p = 0.47$) for the test set. (**b**) Furthermore, a permutation test indicated lack of predictive robustness (95th percentile threshold = 17.38% vs. model RMSE = 23.00). (**c**), For high mental effort (HME) choices, our model showed a strong correlation ($r = 0.5$, $p = 0.034$), underscoring the model's efficacy in anticipating decision patterns based on dmPFC/dACC metabolite profiles. (**d**) Permutation test for HME predictions confirms model accuracy (95th percentile threshold = 13.46% vs. model RMSE = 12.51%). (**e**) Feature importance analysis via SHAP values for HME prediction identifies nine key metabolites: glutamate (Glu), lactate (Lac), glutamine (Gln), glutamate + glutamine (Glx), N-acetylaspartate (NAA), N-acetylaspartylglutamate (NAAG), aspartate (Asp), glutathione (GSH), and phosphocreatine+creatine (PCr + Cr). (**f**) A model trained on AI metabolites' predictive power for HME reveals a negative correlation between predicted and actual HME that does not reach statistical significance ($r = -0.4$, $p = 0.92$). (**g**), A permutation test further indicates a significant deviation in model performance for AI-based predictions (95th percentile threshold = 13.81% vs. model RMSE = 17.88%), highlighting a failure to predict HME choices based on AI metabolites.

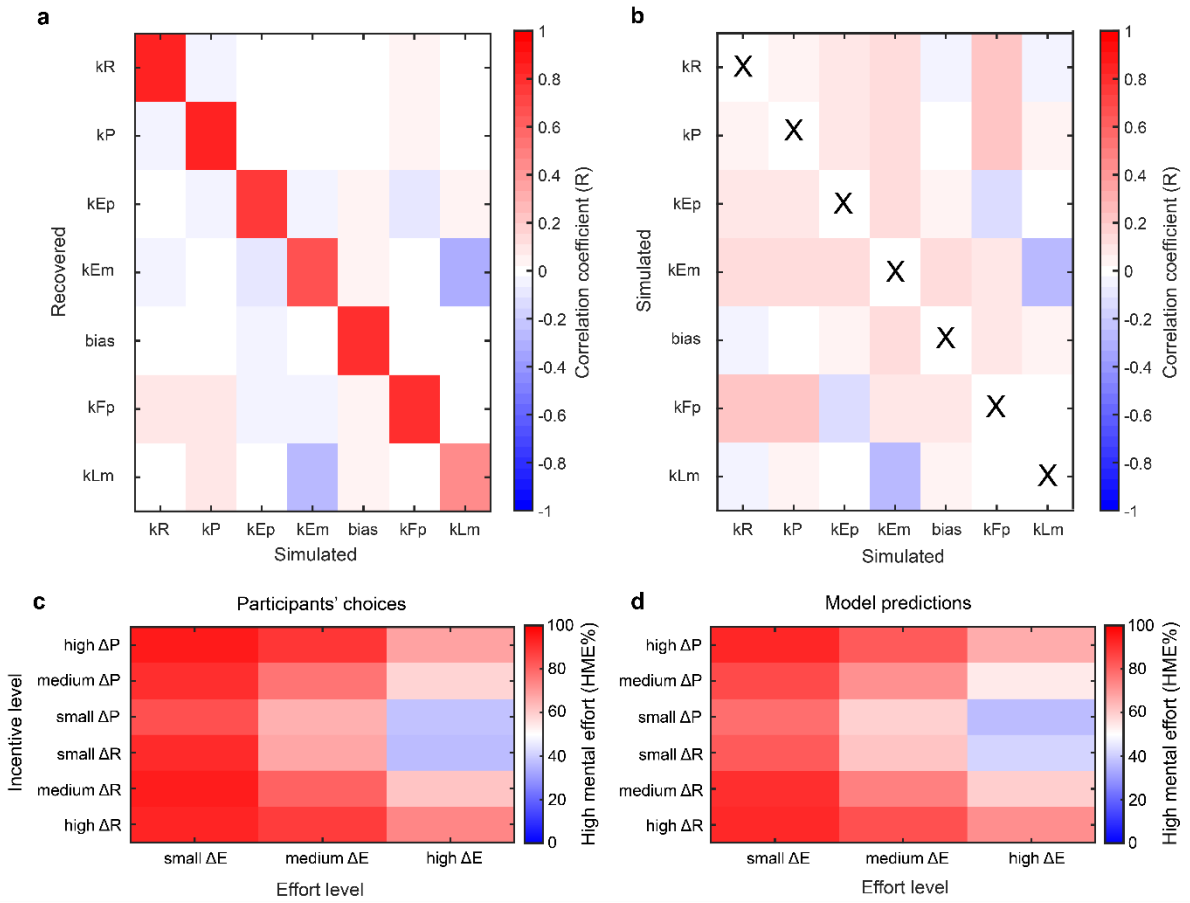

Fig. 3: Comprehensive analysis of model parameters. (**a**) Confusion matrix evaluating the model's parameter recovery capability, contrasting recovered parameters against their original (simulated) counterparts. The parameters correspond to the sensitivity for reward (kR), punishment (kP), physical effort (kEp), mental effort (kEm), a bias toward the high effort option (bias), physical fatigue (kFp) and mental learning (kLm). (**b**) Autocorrelation matrix derived from 30'000 simulations assessing the identifiability of all model parameters. (**c**) Heatmap representing the percentage of high mental effort (HME) choices in function of the difference between the high and the low effort option in terms of effort and incentive levels across participants. (**d**) Corresponding heatmap representing the percentage of high mental effort (HME) choices predicted by our computational model in function of the difference between the high and the low effort option in terms of effort and incentive levels.

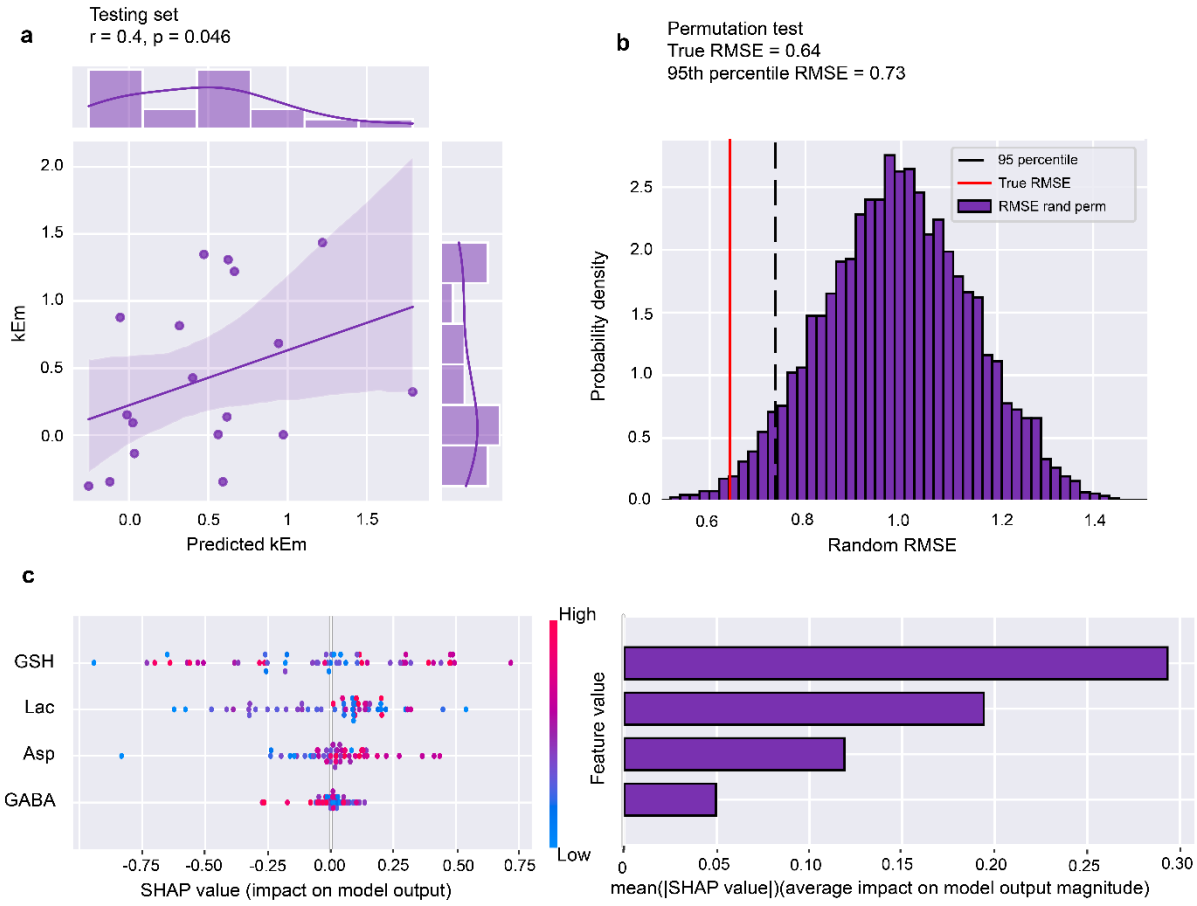

Fig. 4: Assessment of the model's explanatory power for mental effort sensitivity (kEm) using dmPFC/dACC metabolite concentrations. (**a**) A model based on dmPFC/dACC metabolites selected through an automated feature selection process shows a positive correlation (r = 0.40, p = 0.046) between predicted and observed values of kEm based on the XGBoost model's test set performance, highlighting the model's predictive accuracy. (**b**) Histogram of root mean square error (RMSE) from a permutation test involving random label permutation showing a clear validation of the model's robustness. The test and the results reveal that the model's RMSE (0.64) surpasses the 95th percentile of the permuted data (threshold RMSE = 0.73), confirming that the model's predictive success is not due to chance. (**c**) SHAP summary plot representing the impact of each feature on the model output for individual predictions. The analysis identifies five key metabolite parameters— Glutathione (GSH), Lactate (Lac), Aspartate (Asp) and γ-Aminobutyric acid (GABA). Right panel: The horizontal dispersion of SHAP values per feature indicates the variability and influence of each on model predictions.

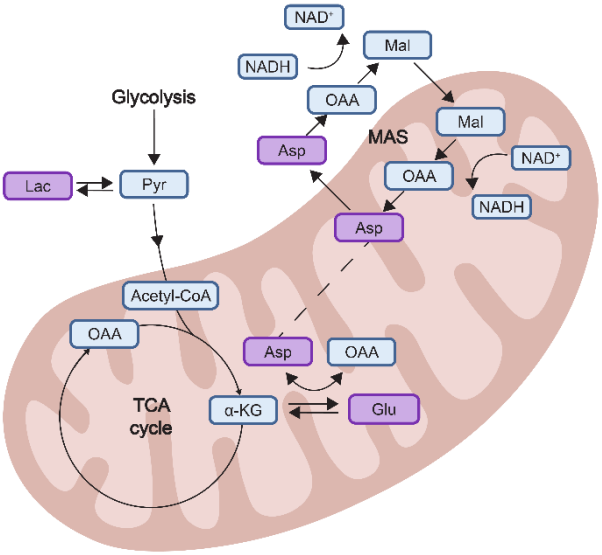

Fig. 5: Schematic representation of the identified metabolites within the tricarboxylic acid (TCA) cycle and the malate-aspartate shuttle (MAS) within mitochondria. The scheme depicts the interplay among key metabolites pertinent to neuronal energy metabolism. Highlighted in bold purple are the key metabolites related to mental effort motivation identified in this study: glutamate (Glu), aspartate (Asp), and lactate (Lac). The diagram traces the pathways of Asp and Glu within the TCA cycle and the role of Lac in glycolysis. Key intermediates include pyruvate (Pyr), alpha-ketoglutarate (α-KG), oxaloacetate (OAA), malate (Mal), and acetyl-CoA, along with the redox couple NAD+/NADH, integral to both the TCA cycle and MAS. This visual abstract underscores the metabolic fluxes that are hypothesized to underpin the cognitive processes.

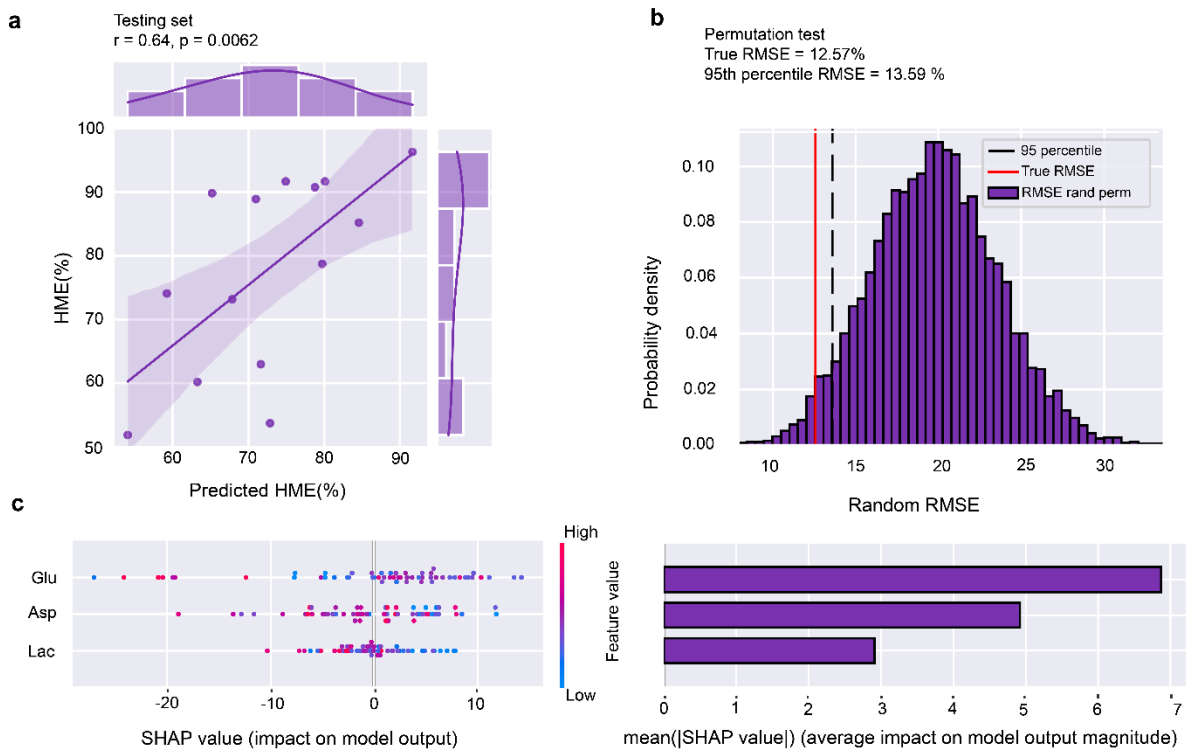

Fig. 6: Model for high mental effort (HME) choices using key metabolites from the dmPFC/dACC. (**a**) A strong positive correlation (r = 0.64, p = 0.0062) between the XGBoost model's predicted probability of HME choices and the observed percentages within the test set, indicating robust predictive validity using the metabolites glutamate (Glu), aspartate (Asp), and lactate (Lac). (**b**) A permutation test that randomizes the labels and recalculates the RMSE to compare against the model's true performance indicates the model's predictive reliability, i.e., the true RMSE of the model (12.57.%) is well below the 95th percentile of the permuted distribution (threshold RMSE = 13.59%), indicating that the model's predictions are not due to random chance. (**c**) SHAP value summary plot depicting the impact of each metabolite on the model's predictions for individual subjects. Right panel: The magnitude and distribution of the SHAP values for glutamate, aspartate, and lactate indicate their respective contributions to the model's decision-making process.